WARSAW UNIVERSITY OF TECHNOLOGY Index 351733
FACULTY OF CIVIL ENGINEERING
COMMITTEE FOR CIVIL AND WATER ENGINEERING
POLISH ACADEMY OF SCIENCES ISSN 1230-2945
DOI: 10.24425/ace.2024.151899
ARCHIVES OF CIVIL ENGINEERING
Vol. LXX ISSUE 4 2024
pp. 391 –405
© 2024. Dorota Krystosik.

This is an open-access article distributed under the terms of the Creative Commons Attribution-NonCommercial-NoDerivatives License (CC BY-NC-ND 4.0, https://creativecommons.org/licenses/by-nc-nd/4.0/), which permits use, distribution, and reproduction in any medium, provided that the Article is properly cited, the use is non-commercial, and no modifications or adaptations are made.

**Research paper**

# Experimental tests of welded knee joints of steel frames

**Dorota Krystosik**[1]

**Abstract:** The paper focuses on presenting the methodology of testing corner joints along with the presentation of obtained results. The objective of the conducted research was to experimentally determine the behaviour of welded knees with slender webs under similar loading condition that occur in the knee joints of portal steel frames. Laboratory tests were carried out on a specially prepared testing stand. During the laboratory work, load tests were performed on three identical knees. The testing stand was equipped with measurement equipment, including two data acquisition systems: the SAD 256 for displacement and force sensors, and the Pontos/Aramis – a digital image correlation system. The first knee test served as a verification of the testing stand and the adopted data collection method. After implementing certain changes to the stand, the remaining load tests on the knees were conducted. Based on the conducted studies and data analysis, moment-rotation $M$–$\phi$ characteristics of the joints were determined, along with parameters such as initial stiffness $S$, elastic bending resistance $M_{\mathrm{el}}$ and ultimate bending resistance $M_{\mathrm{u}}$.

**Keywords:** frame knee, joint, resistance, stiffness

[1]MSc., Eng., Koszalin University of Technology, Faculty of Civil Engineering, Environment and Geodetic Sciences, ul. Śniadeckich 2, 75-453 Koszalin, Poland, e-mail: dorota.krystosik@tu.koszalin.pl ORCID: 0000-0001-5861-8530

# 1. Introduction

The frame knee, also known as a knee joint, or an eaves joint is the connection point between the column and the beam (rafter) of the frame. In engineering practice, joints of this type can be designed as bolted or welded. If certain requirements are met, such as resistance to instability of flat shear plates, this type of joint can be calculated using the component method recommended by Eurocode [1].

In the subject literature, you can find papers that describe the issues of examining welded joints, including those made from hollow sections [2]. There are also a very few research papers that focus on the examination of frame knees with I sections [3].

The proper design of the knee joint is a relatively difficult issue [4–7]. This difficulty primarily arises from the significant internal forces present in the knee and the complex geometry of the joint itself. Designing and dimensioning high-strength joints is often easier in case of welded joints [8]. On the other hand, the connection between the column and the beam at the construction site can be achieved through a bolt connection, placed at a certain distance from the knee, where the internal force values are lower.

The article presented in this paper introduces the methodology and presents the results of testing conducted on the steel knee joints of under static load. During the tests, particular emphasis was placed on evaluating the stiffness and resistance of knees with slender webs. A dedicated testing stand was designed specifically for this purpose to induce the load condition in the tested elements that actually occurs in the knees of steel frames.

The experiment was conducted on three identical knees, with the first one serving as a pilot study to verify the testing stand and measurement methods employed.

# 2. Description of the tested knee

The tested knee adopted for the study consisted of two perpendicular connected I-section beams, ended with end plates. As a result, the main part of the joint formed a square web panel, with all edges supported by flanges and stiffeners (Fig. 1).

The welded connections of the joint components were designed as double-sided fillet welds to ensure the full strength of the connected plates. The web panel had a thickness of 3 mm, while the flanges and stiffeners had a thickness of 8 mm. The end plates of the assembly joints were made of 20 mm thick material. All knees were constructed using S355 steel.

Knees no. 2 and no. 3, which were the focus of the research, underwent an assessment of fabrication accuracy, with special attention given to imperfections or geometric deviations relative to the mid-plane of the knee.

Precise geometric leveling measurements were conducted using the Leica DNA 03 device and an invar bar code to determine the position of selected points within the leveled knee. The sought-after deviation was represented by the difference in coordinates between the knee support and the specific point.

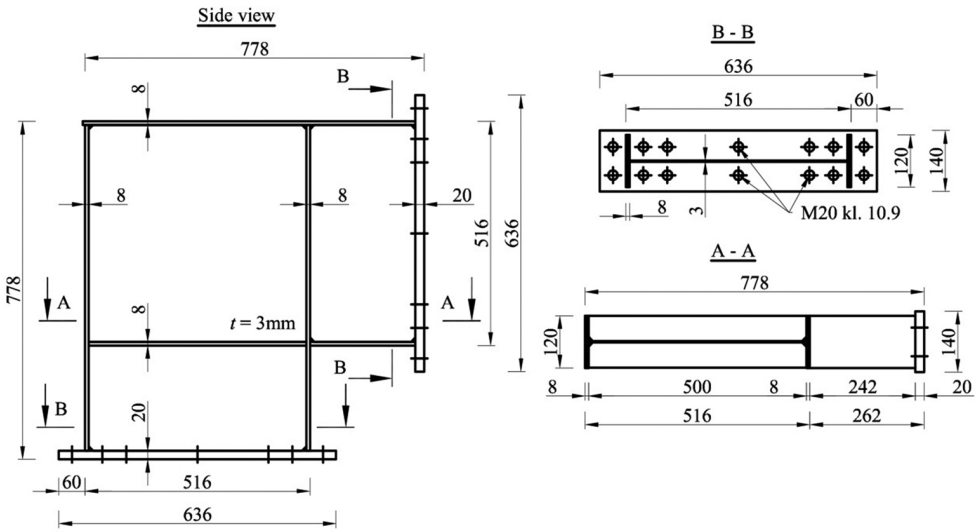


Fig. 1. Geometric and mean dimensions of the tested knees

Multiple measurements were taken for each element within the web and the narrow planes of the flanges, stiffeners, and end plates (Fig. 2). The key results from the analysis of the measurement imperfections are presented in Table 1.

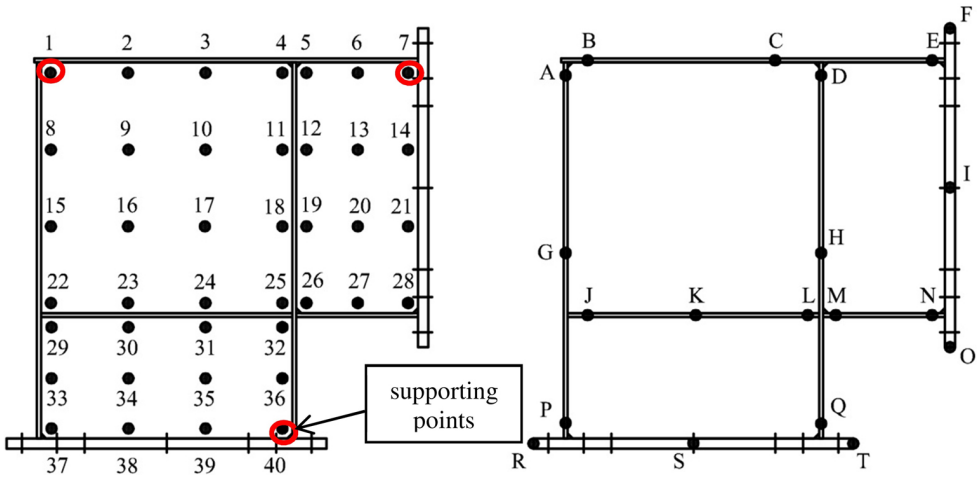


Fig. 2. The positions of measurement points for knee no. 2 and no. 3

Based on the measurement results, it was found that the tested elements exhibited a very high level of fabrication accuracy.

Table 1. Compilation of the most important results from imperfection measurements

| Knee | Web panel deviation | | Deviation of narrow planes of other plates | |
|---|---|---|---|---|
| | average [mm] | maximum [mm] | average [mm] | maximum [mm] |
| no. 2 | 0.085 | 0.302 | 0.020 | 0.684 |
| no. 3 | –0.039 | 0.234 | 0.429 | 0.534 |

## 2.1. Material characteristics of the tested elements

As part of the research program, the mechanical parameters of the material used for the knees were determined. During the prefabrication stage of the joints, samples were taken from the steel sheets for material testing in a static tensile test, according to [9]. A total of 12 samples in the form of "dog-bone" specimens were prepared from 3mm (Group A) and 8 mm (Group B) thick plates. All samples were fractured in the gauge length regions, so no results were discarded in the initial stage of the analysis. Figure 3 presents the stress-strain characteristics ($\sigma$–$\varepsilon$) for samples from both groups, while Tables 2 and 3 provide numerical values of the results.

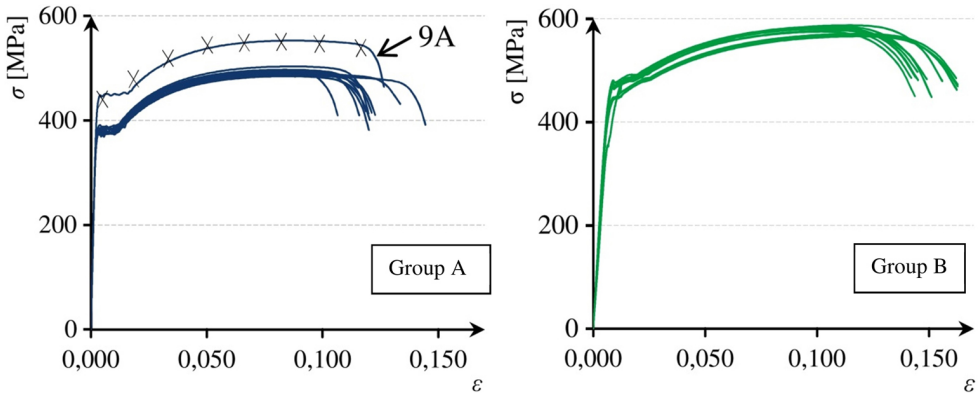


Fig. 3. Stress-strain $\sigma$–$\varepsilon$ characteristics for samples in Group A and B

After analyzing the diagrams ($\sigma$–$\varepsilon$) of both groups, it is evident that the results of one sample in Group A (9A) deviate from the others. Therefore, a statistical test was conducted to reject the individual erroneous measurement, assuming that the test results are random variables following a Gaussian distribution. The criterion for rejecting results with gross errors was based on the three sigma rule described by the formula $|x - x\dot{Z}| \geqslant 3s$, which states that results outside this defined range should be discarded. It was found that the yield strength for the sample labeled as 9A does not fall within the desired range of proper standard deviations.

Hence, the result of the 9A sample was rejected, and the remaining values were used for further calculations. Table 4 presents a summary of the mean values of the obtained results for both groups.

Table 2. Summary of the obtained results for group A

| Sample symbol | Initial cross-sectional area | The largest force | Standard deviation for $F_m$ | Yield strength | Standard deviation for $R_e$ | Young's modulus | Standard deviation for $E$ |
|---|---|---|---|---|---|---|---|
| | $S_o$ [mm$^2$] | $F_m$ [kN] | $s$ [kN] | $R_e$ [MPa] | $s$ [MPa] | $E$ [GPa] | $s$ [GPa] |
| 1A | 45.21 | 22.374 | 0.83 | 385.15 | 20.48 | 193.67 | 3.27 |
| 2A | 45.09 | 22.567 | | 390.32 | | 203.00 | |
| 3A | 43.96 | 22.323 | | 380.46 | | 200.04 | |
| 4A | 45.03 | 21.853 | | 375.78 | | 201.21 | |
| 5A | 44.76 | 22.093 | | 380.90 | | 200.91 | |
| 6A | 44.22 | 22.047 | | 380.32 | | 204.94 | |
| 7A | 44.73 | 21.919 | | 380.74 | | 203.82 | |
| 8A | 44.46 | 22.304 | | 385.12 | | 200.65 | |
| 9A | 44.91 | 24.878 | | 450.30 | | 202.94 | |
| 10A | 43.75 | 21.833 | | 375.98 | | 203.31 | |
| 11A | 44.58 | 22.223 | | 380.78 | | 198.71 | |
| 12A | 44.37 | 21.803 | | 375.17 | | 206.01 | |
| average | 44.59 | 22.350 | – | 386.75 | – | 201.60 | – |
| Standard values for steel S 355 | | | | 355 | | 210 | |

# 3. Description of the testing stand, equipment, and measurement methods

## 3.1. Description of the testing stand

The laboratory tests of the steel frame knees were conducted at the Departmental Laboratory of Materials and Building Structures at Koszalin University of Technology, using a specially prepared testing stand shown in Fig. 4.

The stand consists of two rigid arms connected to the tested knee joint at the upper part. The connections between the knee and the arms of the stand was made using 20 mm thick bed plates and 14 sets of M20 class 10.9 HV bolts on one side. The assembled elements were mounted on two supports: on the left side, a hinge support (with horizontal movement locked during the main part of the test), and on the right side, a roller support. The load applied to the tested knee joint was achieved using hydraulic actuators that exerted a horizontal force in the place where the right arm was supported.

Table 3. Summary of the obtained results for group B

| Sample symbol | Initial cross-sectional area | The largest force | Standard deviation for $F_m$ | Yield strength | Standard deviation for $R_e$ | Young's modulus | Standard deviation for $E$ |
|---|---|---|---|---|---|---|---|
| | $S_o$ [mm$^2$] | $F_m$ [kN] | $s$ [kN] | $R_e$ [MPa] | $s$ [MPa] | $E$ [GPa] | $s$ [GPa] |
| 1B | 233.86 | 140.982 | | 483.15 | | 178.31 | |
| 2B | 235.72 | 138.559 | | 471.18 | | 176.12 | |
| 3B | 233.99 | 135.829 | | 442.14 | | 207.73 | |
| 4B | 235.86 | 140.512 | | 484.78 | | 201.92 | |
| 5B | 234.46 | 137.964 | 1.73 | 475.95 | 15.14 | 199.44 | 13.90 |
| 6B | 236.04 | 136.972 | | 456.34 | | 211.26 | |
| 7B | 235.56 | 139.457 | | 475.90 | | 188.59 | |
| 8B | 234.76 | 136.252 | | 445.86 | | 166.58 | |
| 9B | 234.16 | 139.299 | | 477.48 | | 178.38 | |
| 10B | 233.78 | 139.573 | | 471.15 | | 190.58 | |
| 11B | 235.86 | 140.236 | | 483.22 | | 191.66 | |
| 12B | 235.58 | 136.997 | | 452.22 | | 201.01 | |
| average | 234.97 | 138.553 | – | 468.28 | – | 201.01 | – |
| Standard values for steel S 355 | | | | 355 | | 210 | |

Table 4. Summary of results

| | Yield strains | Yield strength | The larger force | Ultimate strength | Young's modulus |
|---|---|---|---|---|---|
| | $\varepsilon_y$ [%] | $R_e$ [MPa] | $F_m$ [kN] | $R_m$ [MPa] | $E$ [GPa] |
| Group A | 0.02 | 380.98 | 22.12 | 496.65 | 201.49 |
| Group B | 0.02 | 468.28 | 138.55 | 577.03 | 201.01 |

## 3.2. Description of devices and measurement methods

Data recording during the tests was carried out using two independent systems: SAD 256 with a set of integrated sensors and Pontos/Aramis with two cameras.

The first of the mentioned system is a multichannel recorder that allows for simultaneous recording of 47 non-electrical quantities. It works with sensors for measuring deformations, displacements, forces, temperature, and pressure (Fig. 5).

During the tests of the knees, this equipment was used to record data from force sensors (mounted on hydraulic actuators) and displacement sensors, including those on the direction of

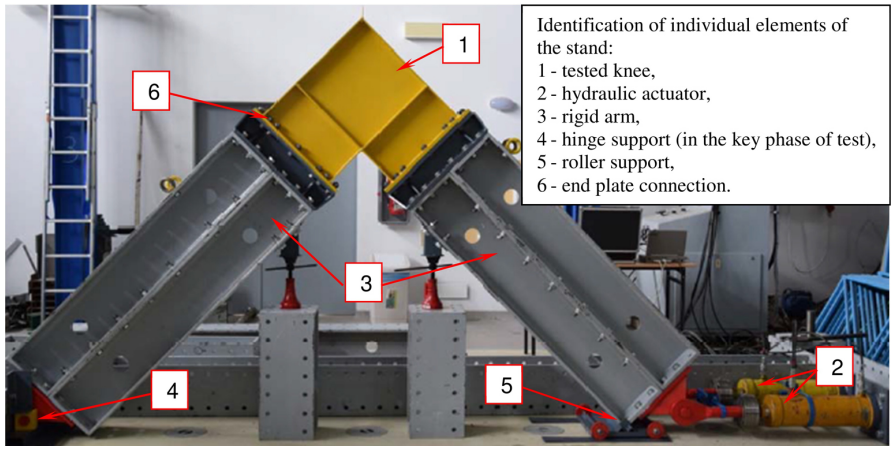


Fig. 4. View of the testing stand

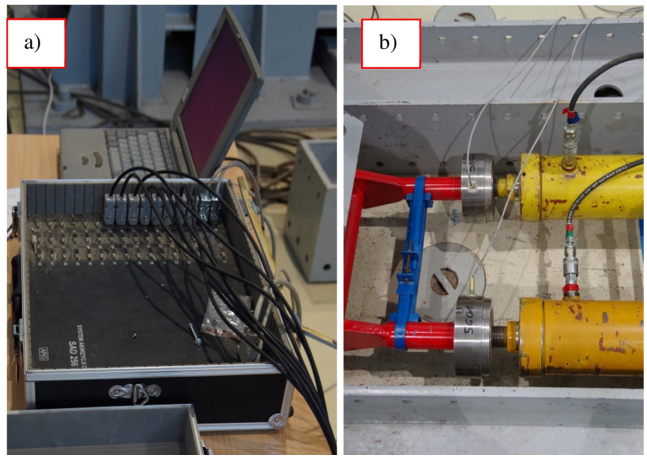


Fig. 5. Equipment of the SAD 256 system: (a) signal analyzer with computer, (b) set of two actuators with force sensors

the applied load. Figure 5b shows a set of two parallel hydraulic actuators with force sensors connected to the data analyzer.

The second method of data recording was based on optoelectronic techniques. During the test, a series of high-resolution photographs were taken at a user-defined frequency. These photographs were then analyzed using specialized software – GOM Correlate [10]. The Pontos/Aramis system can be equipped with one or more cameras. Using a single camera allows for the determination of displacements in a plane parallel to the recorded image, while two cameras enable the measurement of deformations in three-dimensional space.

The process of image processing primarily involves digital image correlation. It involves the comparative analysis of images in the initial state (state 0) and the current state (state $i$).

One of the images, typically the image of the object before loading, is chosen as the reference image. A regular grid of points is placed on this image within a defined area (contour). Each point represents the center of a square or rectangular area (called a facet) with side dimensions ranging from several to several tens of pixels. Each facet is assigned coordinates in the adopted reference system (which can be determined during the system calibration). During the analysis, the software compares the current state image with the reference image, thereby determining the deformations of the facets. The obtained information can be used to create displacement vectors of selected points, an intensity image of strains, or the actual deformation of the surface of the tested object [10].

After conducting the initial study to verify the testing stand and measurement equipment, certain changes were introduced that, in the author's opinion, positively influenced the subsequent tests. The most important changes that significantly improved the quality of the obtained results include:

- using low-gloss paint (for both the background and contrasting pattern) on the surface of the tested elements. This significantly reduced reflections on the photographed surfaces,
- adjusting the camera setup relative to the tested knee joint and proper object illumination. This allowed the GOM Correlate software to apply a denser point grid across the entire surface of the joint, resulting in more comprehensive information about displacements in this area,
- modifying the design of lateral bracing that determines the position of the knee joint in the vertical plane and provides stability during the test. The tension members (Fig. 6a) were replaced with rolling elements moving along defined, rigid planes (Fig. 6b),
- making a change in the support conditions of the testing stand. During the initial loading phase, the left support functioned as a rolling support (using spacers to minimize frictional forces), while in the crucial stage, it acted as a pined, immovable support (allowing for precise determination of the forces acting on the system during the initial and main phases of the test).

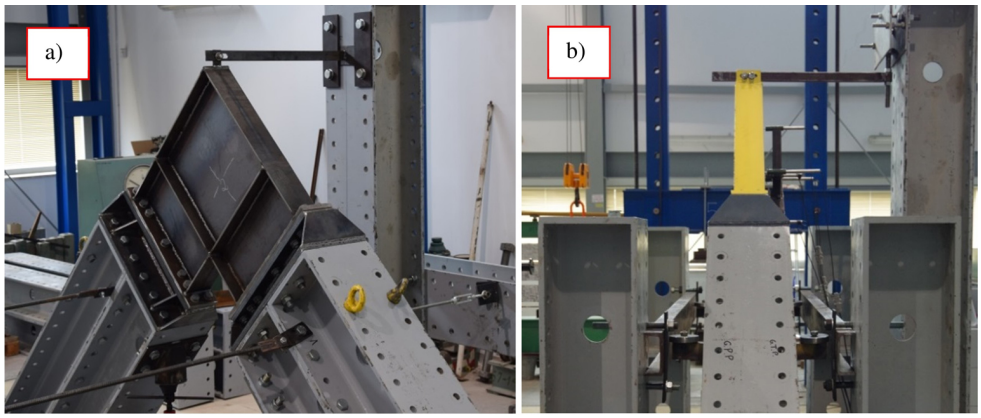


Fig. 6. Bracing system in the testing stand: (a) bracing achieved using tension members, (b) bracing achieved using rollers moving along defined, rigid planes

# 4. Analysis of knees test results

The first stage of analyzing the test results involved determining the internal forces (particularly the bending moment M) at the corners. These forces were determined based on measurement data from the SAD 256 system. By considering the system of forces acting on the testing stand (Fig. 7a), it was easy to determine the internal force values at the examined knee (Fig. 7b).

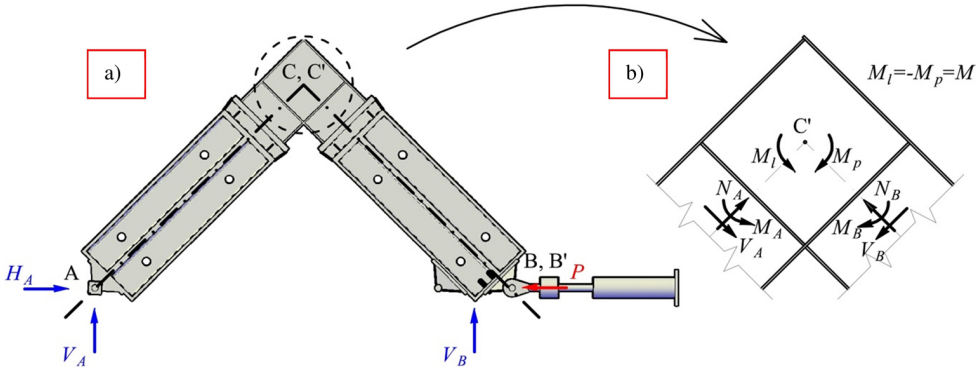


Fig. 7. The knee under load: (a) external force system, (b) internal force system

However, it should be noted that under the influence of loading, certain changes occur in the geometry of the stand. This effect is schematically presented in Fig. 8, with the solid line indicating the initial state of the system (state 0) and the dashed line indicating the current state ($i$-th). It should be emphasized that significant changes in geometry occur when individual node zones undergo substantial deformation.

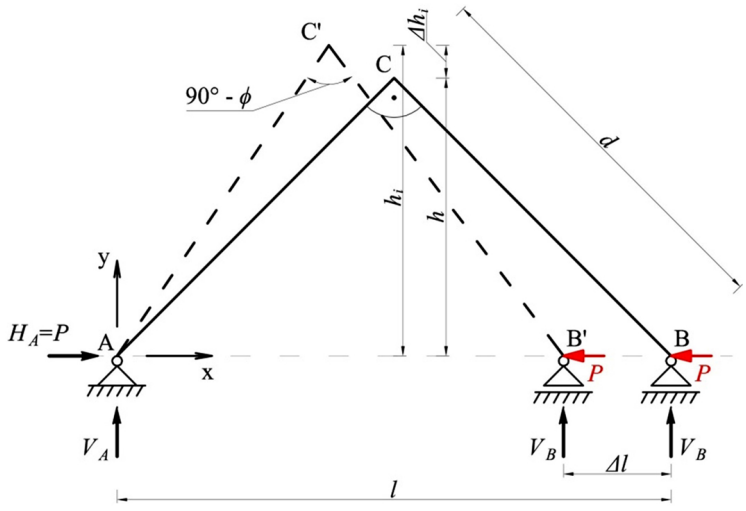


Fig. 8. Change in geometry of the stand elements under the influence of applied load

These changes somewhat affect the force values at the joint. Therefore, based on the geometric relationships between the two distinguished states, the value of the bending moment $M_i$ at the knee was determined according to the formula:

$$M_i = P_i \cdot h_i = P_i \cdot \sqrt{d^2 - \left(\frac{l - \Delta l_i}{2}\right)^2} - V_A \cdot \frac{l - \Delta l_i}{2} \tag{4.1}$$

where: $\Delta l_i$ is the average displacement measured using 2 displacement sensors along the axes of the actuators, and $P_i$ is the sum of horizontal forces measured using force sensors.

The second stage of data analysis involved determining the deformations of the tested knees based on the collected data using the Pontos/Aramis system. The main geometric quantity of interest was the change in the angle between the arms of the knee. Photographs (Fig. 9a–c) depict images of the knee with the angles $\alpha_i$ determined using GOM Correlate software. The reference lines were established within the knee areas where no significant deformations were observed. The first photograph (Fig. 9a) was selected as the reference state before applying the load, the second photograph (Fig. 9b) represented a randomly chosen image of the knee under load, and the third photograph (Fig. 9c) was the last one recorded during the test.

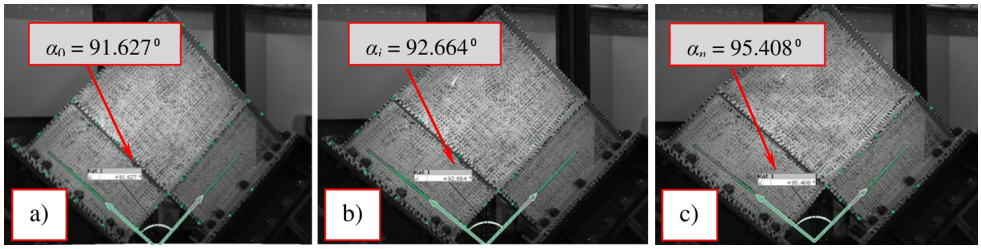


Fig. 9. Photos of the knee: (a) knee before loading, (b) randomly selected view of the knee under load, (c) knee deformation after the test

Based on the collected and processed information, a set of angle $\phi$ values was determined for each tested knee according to the equation:

$$\varphi_i = \alpha_i - \alpha_0, \quad \text{for} \quad i = 1, 2, \ldots, n \tag{4.2}$$

Integrating the data from the first two main stages of the test results analysis allowed the characterization of the moment-rotation ($M_i - -\phi_i$) behavior of the knees. This behavior was approximated using the four-parameter Richard-Abbott power model [11] through the least squares method:

$$M(\varphi) = \frac{(S - S_p) \cdot \varphi}{\left[1 + \left(\frac{S - S_p}{M_\mathrm{u}}\varphi\right)^c\right]^{\frac{1}{c}}} + S_p \cdot \varphi \tag{4.3}$$

where: $S$ represents the initial rotational stiffness, $S_p$ is the rotational strain-hardening stiffness, $M_\mathrm{u}$ is the ultimate bending resistance, and $c$ is the curve-fitting parameter.

Additionally, a linear characteristic of the tested knees describing their behaviour in the initial phase of loading was established with the relationship:

$$M'(\varphi) = S \cdot \varphi \tag{4.4}$$

Numerical parameter values for the corners are presented in Table 5, and the graphical representation of the moment-rotation relationship for all tested knees is shown in Figure 10.

Table 5. Tabular summary of the constant parameters in Formula (4.3)

| Knee no. | The initial stiffness due to rotation | Strain-hardening stiffness | Resistance due to bending | Curve-fitting parameter | Correlation coefficient | Mean squared error |
|---|---|---|---|---|---|---|
| | $S_j$ [kN·m/rad] | $S_p$ [kN·m/rad] | $M_u$ [kN· m] | $c$ | $R$ | $MSE$ |
| 1 | 31 673 | 231.6 | 151.01 | 3.28 | 0.738 | 0.0002 |
| 2 | 28 107 | 550.0 | 146.35 | 3.81 | 0.774 | 0.0002 |
| 3 | 31 186 | 115.9 | 147.67 | 4.20 | 0.702 | 0.0002 |

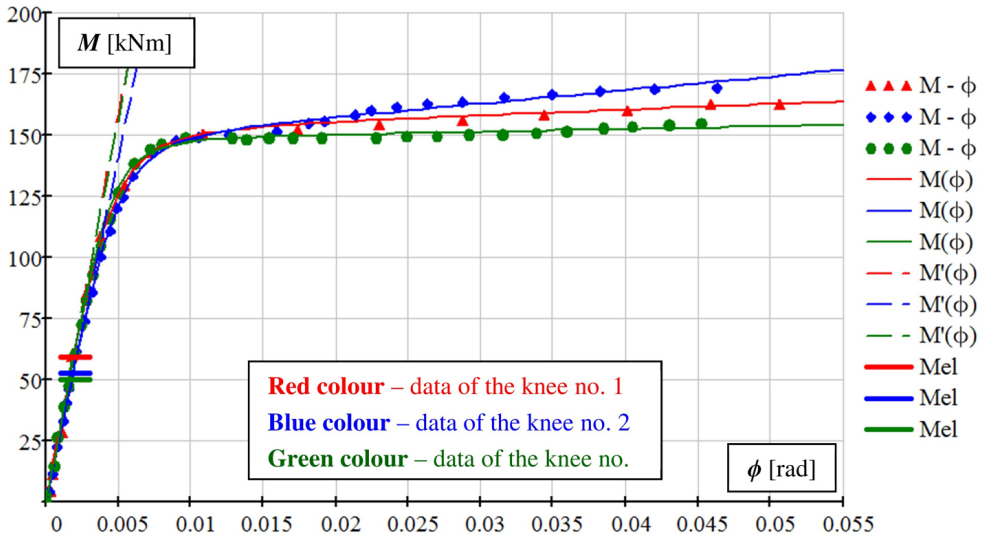


Fig. 10. Moment – rotation characteristics of the all tested knees

The adoption of slender webs significantly influenced the course of the $M--\phi$ relationship for the tested knee joints. Therefore, bending moments $M_{el}$ at the knees were determined beyond which the web panels experienced buckling. The identification of $M_{el}$ was performed

based on the results of the photogrammetric analysis of the knee images using GOM Correlate software. Based on the data of increasing deformations of the knees under load, the value of angle $\phi_{el}$ was identified, which corresponded to the appearance of perpendicular displacements to the web (Fig. 11 and 12).

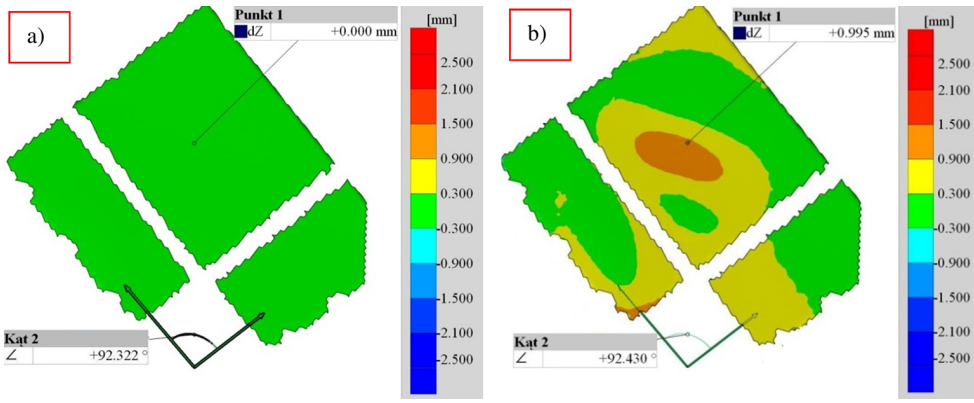


Fig. 11. Perpendicular displacements to the web: (a) image depicting the state 0 – before knee loading, (b) displacements from the "initiating" instability-inducing load of the web

The values of angles $\phi_{el}$ and the analytical characteristics $M(\phi)$ were then used to determine the numerical values of moments $M_{\text{el}}$. The results are presented in Table 6 and plotted on the $M - -\phi$ dependency graphs (Fig. 10).

Table 6. Compilation of the angles $\phi_{el}$ and the corresponding moments $M_{\text{el}}$

| **Knee no.** | **Angle value** | **Bending moment** |
|---|---|---|
| | $\boldsymbol{\phi_{el}}$ **[rad]** | $\boldsymbol{M_{el}}$ **[kN· m]** |
| 1 | 0.0019 | 59.34 |
| 2 | 0.0019 | 52.58 |
| 3 | 0.0016 | 49.78 |

Additionally, utilizing the capabilities of the GOM Correlate software, the main strains in the webs of the knees under load were determined, which corresponded to the load initiating stability loss (Fig. 12).

The strains values averaged at 0.12%, which is below 0.2% (see Table 4). This indicates that the occurrence of transverse deformations in the webs took place at stress levels lower than the yield strength of the steel.

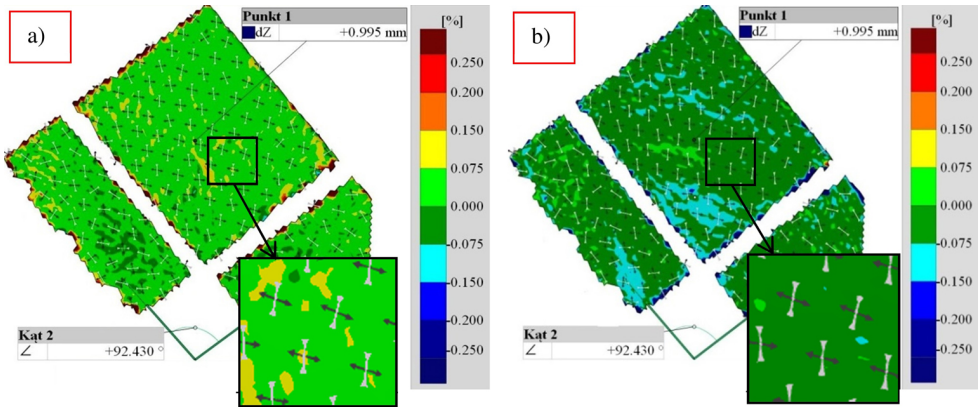


Fig. 12. Deformations in the web panel for the loaded condition (from Fig. 11b): (a) principal strains I (under tension), (b) principal strains II (under compression)

# 5. Conclusions

The aim of the presented experimental studies was to determine the behaviour of steel knee joints with slender web under static load. The study was conducted on three identical welded knees. In each of the tested knees, the failure mode was very similar – under the influence of the increasing load, the knee webs buckled in elastic range.

Despite some differences observed between the preliminary test (performed on knee no. 1) and the tests on the other two knees, significant similarities in the $M$–$\phi$ characteristics can be observed. This is believed to be due to the high precision of the test specimens' fabrication and the repeatability of the testing conditions.

The presented method of joint testing, experimental data recording, and the adopted methods of result analysis enable a detailed determination of the behavior of the knee joints, both in the initial and final stages of loading. This is possible even when the tested joints exhibit sensitivity to the loss of stability of individual components (e.g., web panels). Furthermore, the prepared testing setup allows for the examination of corners with different geometries.

However, it is important to emphasize that these are studies that require further, detailed analysis. Nevertheless, the adopted research methodology and the method of result recording suggest that the proposed approach to examining joints is appropriate.

The objective of these studies is to gain a better understanding of the behavior of welded knee joints under load, which will contribute to the development of more rational methods for their design in the future.

## References

[1] EN 1993-1-8:2005 Eurocode 3: Design of steel structures -Part 1–8: Design of joints.

[2] T. Wilkinson and G. J. Hancock, *Tests Of Knee Joints In Cold-Formed Rectangular Hollow Sections. Research Report No R779.* Sydney, Australia: University of Sydney 1998.

[3] I. Vayas, J. Ermopoulos, and H. Pasternak, "Design of Steel Frames with Slender Joint-panels", *Journal of Constructional Steel Research*, vol 35, no. 2, pp. 165–187, 1995, doi: 10.1016/0143-974X(94)00034-F.

[4] The Steel Construction Institute, *Publication P398: Joints in Steel Construction: Moment-resisting Joints to Eurocode 3*. The Steel Construction Institute, 2013.

[5] A. Kozłowski and Z. Pisarek, "End-plate steel joint with four bolts in the row", presented at XI International Conference on Metal Structures, (ICMS-2006), Rzeszów, Poland, 21–23 June 2006.

[6] L. Ślęczka, *Shaping and analysis of selected steel frame joints subjected to variable actions*. Oficyna Wydawnicza Politechniki Rzeszowskiej, 2013 (in Polish).

[7] K. Urbonas and A. Daniūnas, "Component method extension to steel beam-to-beam and beam-to-column knee joints under bending and axial forces", *Journal of Civil Engineering and Management*, vol. 11, no. 3, pp. 217–224, 2005, doi: 10.3846/13923730.2005.9636353.

[8] P. Krystosik, "Design resistance of welded knees in steel frames", *Journal of Civil Engineering, Environment and Architecture*, vol. 35, no. 65, pp. 115–132, 2018, doi: https://bibliotekanauki.pl/articles/104292.

[9] EN ISO 6892-1:2019 Metallic materials -Tensile testing – Part 1: Method of test at room temperature.

[10] *GOM Correlate V8 SR1 Manual Basic*. Braunschweig, Germany, 2015.

[11] W. F. Chen, N. Kishi, and M. Komuro, *Semi-rigid connection handbook*. J. Ross Publishing, 2011.

## Badania doświadczalne spawanych naroży ram stalowych

**Słowa kluczowe:** naroże ramy, węzeł, nośność, sztywność

### Streszczenie:

Naroże ramy stalowej, nazywane również węzłem narożnym, bądź okapowym, jest miejscem połączenia słupa oraz rygla ramy. W praktyce inżynierskiej węzły tego typu można projektować jako śrubowe bądź spawane. Przy spełnieniu pewnych wymagań (dotyczących np. odporności na niestateczność płaskich, ścinanych ścianek), węzły tego typu można obliczać zalecaną przez EC3 metodą składnikową. Tematem niniejszej pracy jest przedstawienie metodyki badań naroży ram o smukłych, wrażliwych na wyboczenie środnikach, wraz z prezentacją otrzymanych wyników. Do badań przyjęto węzełnarożny, w którym pod kątem prostym połączono dwa dwuteowe króćce blachownicowe, zakończone grubymi blachami węzłowymi. W efekcie, zasadnicza część węzła przyjęła postać kwadratowego panelu środnika, którego wszystkie krawędzie są podparte pasami oraz żebrami usztywniającymi. W ramach przyjętego programu badań określono parametry mechaniczne materiału, z którego wykonano naroża. Na etapie prefabrykacji węzłów, z arkuszy blach pobrano próbki do badań materiału w statycznej próbie rozciągania. Ponadto, naroża poddano ocenie dokładności wykonania, ze szczególnym uwzględnieniem imperfekcji (odchyłek geometrycznych) względem płaszczyzny środkowej naroża. Pomiary wykonano metodą geometrycznej niwelacji precyzyjnej, określając położenie wybranych punktów wypoziomowanego naroża. Różnica rzędnych: podparcia naroża oraz danego punku, stanowiła poszukiwaną odchyłkę. Zasadnicze badania przeprowadzono na trzech jednakowych narożach spawanych, na specjalnie przygotowanym do tego celu stanowisku badawczym. Stanowisko to składało się z dwóch sztywnych ramion, które w górnej części połączono badanym węzłem narożnym. Scalone elementy osadzono na dwóch podporach: z lewej strony na podporze przegubowo nieprzesuwnej (w zasadniczej części badania z blokadą przesuwu poziomego), z prawej strony na podporze przegubowo przesuwnej. Obciążenie dział ające na badane naroże ramy uzyskano przy użyciu siłowników hydraulicznych, które wywierały siłę poziomą w miejscu podparcia prawego ramienia. Zapis danych podczas trwania badań odbywał się przy użyciu dwóch niezależnie działających systemów: SAD 256 z zestawem zintegrowanych czujników oraz Pontos/Aramis wraz z dwoma kamerami. Pierwszy z wymienionych systemów jest wielokanałowym rejestratorem

umożliwiającym równoległą rejestrację wielkości nieelektrycznych. Podczas przeprowadzania badań narożу wykorzystano tę aparaturę do zapisu danych z czujników sił (zamontowanych na siłownikach hydraulicznych) oraz czujników rejestrujących przemieszczenia, m. in. na kierunku zadawanego obciążenia. Drugi sposób rejestracji danych bazował na metodach optyczno-elektronicznych. Podczas badania aparatura wykonuje serię zdjęć. Ich rejestracja, w wysokiej rozdzielczości, odbywa się z zadaną przez użytkownika częstotliwością. Następnie fotografie są analizowane przy użyciu specjalistycznego oprogramowania – GOM Correlate. Przeprowadzenie badań niszczących narożу dostarczyło dużej ilości danych. Pierwszy etap analizy wyników polegał na określeniu sił wewnętrznych (w szczególności momentu zginającego $M$) w narożach. Siły te określono na podstawie danych pomiarowych z systemu SAD 256. Drugi etap analizy danych polegał na określeniu deformacji badanych narożу na podstawie zebranych danych przy użyciu systemu Pontos/Aramis. Główną poszukiwaną wielkością geometryczną była zmiana kąta pomiędzy ramionami narożу $\phi$. Integracja danych z dwóch pierwszych, zasadniczych etapów prac nad danymi z badań pozwoliła określić charakterystykę moment–obrót $M$–$\phi$ narożу, które aproksymowano (przy użyciu metody najmniejszych różnic kwadratów) czteroparametrowym modelem potęgowym. Bardzo istotny wpływ na przebieg zależności $M$–$\phi$ badanych narożу miało przyjęcie smukłych środników. Z tego względu, dodatkowo wyznaczono momenty zginające $M_{el}$ w narożach, po przekroczeniu których panele środników ulegały wyboczeniu. Przedstawiony sposób badania węzłów, rejestracji danych eksperymentalnych oraz przyjętych metod analizy wyników dają możliwość dokładnego określenia zachowanie się naroża, zarówno w początkowej, jak i w końcowej fazie obciążenia. Jest to możliwe nawet wtedy, gdy badane węzły odznaczają się wrażliwością na utratę stateczności poszczególnych składników (np. paneli środnika). Ponadto, przygotowane stanowisko badawcze daje możliwość badania narożу o różnej geometrii.Przedmiotowe badania mają na celu lepsze poznanie zachowania się spawanych narożу ram pod obciążeniem, co w przyszłości pozwoli opracować bardziej racjonalne metody ich projektowania.

Received: 2023-11-07, Revised: 2023-12-05